Search for CP violation in the decay $Z \to b\bar{b}g$

D. Buskulic, I. de Bonis, D. Decamp, P. Ghez, C. Goy, J.P. Lees, A. Lucotte, M.N. Minard, J.Y. Nief, P. Odier, et al.

EUROPEAN LABORATORY FOR PARTICLE PHYSICS (CERN)

CERN-PPE/96-71
23 May 1996

Search for $\mathcal{CP}$ Violation in the Decay $Z \to b\bar{b}g$

The ALEPH Collaboration

Abstract

About three million hadronic decays of the Z collected by ALEPH in the years 1991 to 1994 are used to search for anomalous $\mathcal{CP}$ violation beyond the Standard Model in the decay $Z \to b\bar{b}g$. The study is performed by analyzing angular correlations between the two quarks and the gluon in three-jet events and by measuring the differential two-jet rate. No signal of $\mathcal{CP}$ violation is found. For the combinations of anomalous $\mathcal{CP}$ violating couplings, $\hat{h}_b = \hat{h}_{Ab} g_{Vb} - \hat{h}_{Vb} g_{Ab}$ and $h_b^* = \sqrt{\hat{h}_{Vb}^2 + \hat{h}_{Ab}^2}$, limits of $\mid \hat{h}_b \mid < 0.59$ and $h_b^* < 3.02$ are given at 95% CL.

(Submitted to Physics Letters B)

The ALEPH Collaboration

D. Buskulic, I. De Bonis, D. Decamp, P. Ghez, C. Goy, J.-P. Lees, A. Lucotte, M.-N. Minard, J.-Y. Nief, P. Odier, B. Pietrzyk

Laboratoire de Physique des Particules (LAPP), IN^{2}P^3-CNRS, 74019 Annecy-le-Vieux Cedex, France

M.P. Casado, M. Chmeissani, J.M. Crespo, M. Delfino, I. Efthymiopoulos,[1] E. Fernandez, M. Fernandez-Bosman, Ll. Garrido,[15] A. Juste, M. Martinez, S. Orteu, C. Padilla, I.C. Park, A. Pascual, J.A. Perlas, I. Riu, F. Sanchez, F. Teubert

Institut de Fisica d'Altes Energies, Universitat Autonoma de Barcelona, 08193 Bellaterra (Barcelona), Spain[7]

A. Colaleo, D. Creanza, M. de Palma, G. Gelao, M. Girone, G. Iaselli, G. Maggi,[3] M. Maggi, N. Marinelli, S. Nuzzo, A. Ranieri, G. Raso, F. Ruggieri, G. Selvaggi, L. Silvestris, P. Tempesta, G. Zito

Dipartimento di Fisica, INFN Sezione di Bari, 70126 Bari, Italy

X. Huang, J. Lin, Q. Ouyang, T. Wang, Y. Xie, R. Xu, S. Xue, J. Zhang, L. Zhang, W. Zhao

Institute of High-Energy Physics, Academia Sinica, Beijing, The People's Republic of China[8]

R. Alemany, A.O. Bazarko, G. Bonvicini,[23] M. Cattaneo, P. Comas, P. Coyle, H. Drevermann, R.W. Forty, M. Frank, R. Hagelberg, J. Harvey, P. Janot, B. Jost, E. Kneringer, J. Knobloch, I. Lehraus, G. Lutters, E.B. Martin, P. Mato, A. Minten, R. Miquel, Ll.M. Mir,[2] L. Moneta, T. Oest,[20] A. Pacheco, J.-F. Pusztaszeri, F. Ranjard, P. Rensing,[12] L. Rolandi, D. Schlatter, M. Schmelling,[24] M. Schmitt, O. Schneider, W. Tejessy, I.R. Tomalin, A. Venturi, H. Wachsmuth, A. Wagner

European Laboratory for Particle Physics (CERN), 1211 Geneva 23, Switzerland

Z. Ajaltouni, A. Barrès, C. Boyer, A. Falvard, P. Gay, C . Guicheney, P. Henrard, J. Jousset, B. Michel, S. Monteil, J-C. Montret, D. Pallin, P. Perret, F. Podlyski, J. Proriol, P. Rosnet, J.-M. Rossignol

Laboratoire de Physique Corpusculaire, Université Blaise Pascal, IN^{2}P^3-CNRS, Clermont-Ferrand, 63177 Aubière, France

T. Fearnley, J.B. Hansen, J.D. Hansen, J.R. Hansen, P.H. Hansen, B.S. Nilsson, B. Rensch, A. Wäänänen

Niels Bohr Institute, 2100 Copenhagen, Denmark[9]

A. Kyriakis, C. Markou, E. Simopoulou, I. Siotis, A. Vayaki, K. Zachariadou

Nuclear Research Center Demokritos (NRCD), Athens, Greece

A. Blondel, G. Bonneaud, J.C. Brient, P. Bourdon, A. Rougé, M. Rumpf, A. Valassi,[6] M. Verderi, H. Videau[21]

Laboratoire de Physique Nucléaire et des Hautes Energies, Ecole Polytechnique, IN^{2}P^3-CNRS, 91128 Palaiseau Cedex, France

D.J. Candlin, M.I. Parsons

Department of Physics, University of Edinburgh, Edinburgh EH9 3JZ, United Kingdom[10]

E. Focardi,[21] G. Parrini

Dipartimento di Fisica, Università di Firenze, INFN Sezione di Firenze, 50125 Firenze, Italy

M. Corden, C. Georgiopoulos, D.E. Jaffe

Supercomputer Computations Research Institute, Florida State University, Tallahassee, FL 32306-4052, USA[13,14]

A. Antonelli, G. Bencivenni, G. Bologna,[4] F. Bossi, P. Campana, G. Capon, D. Casper, V. Chiarella, G. Felici, P. Laurelli, G. Mannocchi,[5] F. Murtas, G.P. Murtas, L. Passalacqua, M. Pepe-Altarelli

Laboratori Nazionali dell'INFN (LNF-INFN), 00044 Frascati, Italy

L. Curtis, S.J. Dorris, A.W. Halley, I.G. Knowles, J.G. Lynch, V. O'Shea, C. Raine, P. Reeves, J.M. Scarr, K. Smith, P. Teixeira-Dias, A.S. Thompson, F. Thomson, S. Thorn, R.M. Turnbull

Department of Physics and Astronomy, University of Glasgow, Glasgow G12 8QQ,United Kingdom[10]

U. Becker, S. Dhamotharan, C. Geweniger, G. Graefe, P. Hanke, G. Hansper, V. Hepp, E.E. Kluge, A. Putzer, M. Schmidt, J. Sommer, H. Stenzel, K. Tittel, S. Werner, M. Wunsch

Institut für Hochenergiephysik, Universität Heidelberg, 69120 Heidelberg, Fed. Rep. of Germany[16]

D. Abbaneo, R. Beuselinck, D.M. Binnie, W. Cameron, P.J. Dornan, A. Moutoussi, J. Nash, J.K. Sedgbeer, A.M. Stacey, M.D. Williams

Department of Physics, Imperial College, London SW7 2BZ, United Kingdom[10]

G. Dissertori, P. Girtler, D. Kuhn, G. Rudolph

Institut für Experimentalphysik, Universität Innsbruck, 6020 Innsbruck, Austria[18]

A.P. Betteridge, C.K. Bowdery, P. Colrain, G. Crawford, A.J. Finch, F. Foster, G. Hughes, T. Sloan, M.I. Williams

Department of Physics, University of Lancaster, Lancaster LA1 4YB, United Kingdom[10]

A. Galla, I. Giehl, A.M. Greene, K. Kleinknecht, G. Quast, B. Renk, E. Rohne, H.-G. Sander, P. van Gemmeren C. Zeitnitz

Institut für Physik, Universität Mainz, 55099 Mainz, Fed. Rep. of Germany[16]

J.J. Aubert,[21] A.M. Bencheikh, C. Benchouk, A. Bonissent, G. Bujosa, D. Calvet, J. Carr, C. Diaconu, F. Etienne, N. Konstantinidis, P. Payre, D. Rousseau, M. Talby, A. Sadouki, M. Thulasidas, K. Trabelsi

Centre de Physique des Particules, Faculté des Sciences de Luminy, IN^{2}P^3-CNRS, 13288 Marseille, France

M. Aleppo, F. Ragusa[21]

Dipartimento di Fisica, Università di Milano e INFN Sezione di Milano, 20133 Milano, Italy

I. Abt, R. Assmann, C. Bauer, W. Blum, H. Dietl, F. Dydak,[21] G. Ganis, C. Gotzhein, K. Jakobs, H. Kroha, G. Lütjens, G. Lutz, W. Männer, H.-G. Moser, R. Richter, A. Rosado-Schlosser, S. Schael, R. Settles, H. Seywerd, R. St. Denis, W. Wiedenmann, G. Wolf

Max-Planck-Institut für Physik, Werner-Heisenberg-Institut, 80805 München, Fed. Rep. of Germany[16]

J. Boucrot, O. Callot, Y. Choi,[26] A. Cordier, M. Davier, L. Duflot, J.-F. Grivaz, Ph. Heusse, A. Höcker, M. Jacquet, D.W. Kim,[19] F. Le Diberder, J. Lefrançois, A.-M. Lutz, I. Nikolic, H.J. Park,[19] M.-H. Schune, S. Simion, J.-J. Veillet, I. Videau, D. Zerwas

Laboratoire de l'Accélérateur Linéaire, Université de Paris-Sud, IN^{2}P^3-CNRS, 91405 Orsay Cedex, France

P. Azzurri, G. Bagliesi, G. Batignani, S. Bettarini, C. Bozzi, G. Calderini, M. Carpinelli, M.A. Ciocci, V. Ciulli, R. Dell'Orso, R. Fantechi, I. Ferrante, L. Foà,[1] F. Forti, A. Giassi, M.A. Giorgi, A. Gregorio, F. Ligabue, A. Lusiani, P.S. Marrocchesi, A. Messineo, F. Palla, G. Rizzo, G. Sanguinetti, A. Sciabà, P. Spagnolo, J. Steinberger, R. Tenchini, G. Tonelli,[25] C. Vannini, P.G. Verdini, J. Walsh

Dipartimento di Fisica dell'Università, INFN Sezione di Pisa, e Scuola Normale Superiore, 56010 Pisa, Italy

G.A. Blair, L.M. Bryant, F. Cerutti, J.T. Chambers, Y. Gao, M.G. Green, T. Medcalf, P. Perrodo, J.A. Strong, J.H. von Wimmersperg-Toeller

Department of Physics, Royal Holloway & Bedford New College, University of London, Surrey TW20 OEX, United Kingdom[10]

D.R. Botterill, R.W. Clifft, T.R. Edgecock, S. Haywood, P. Maley, P.R. Norton, J.C. Thompson, A.E. Wright

Particle Physics Dept., Rutherford Appleton Laboratory, Chilton, Didcot, Oxon OX11 OQX, United Kingdom[10]

B. Bloch-Devaux, P. Colas, S. Emery, W. Kozanecki, E. Lançon, M.C. Lemaire, E. Locci, B. Marx, P. Perez, J. Rander, J.-F. Renardy, A. Roussarie, J.-P. Schuller, J. Schwindling, A. Trabelsi, B. Vallage

CEA, DAPNIA/Service de Physique des Particules, CE-Saclay, 91191 Gif-sur-Yvette Cedex, France[17]

S.N. Black, J.H. Dann, R.P. Johnson, H.Y. Kim, A.M. Litke, M.A. McNeil, G. Taylor

Institute for Particle Physics, University of California at Santa Cruz, Santa Cruz, CA 95064, USA[22]

C.N. Booth, R. Boswell, C.A.J. Brew, S. Cartwright, F. Combley, A. Koksal, M. Letho, W.M. Newton, J. Reeve, L.F. Thompson

Department of Physics, University of Sheffield, Sheffield S3 7RH, United Kingdom[10]

A. Böhrer, S. Brandt, V. Büscher, G. Cowan, C. Grupen, J. Minguet-Rodriguez, F. Rivera, P. Saraiva, L. Smolik, F. Stephan,

Fachbereich Physik, Universität Siegen, 57068 Siegen, Fed. Rep. of Germany[16]

M. Apollonio, L. Bosisio, R. Della Marina, G. Giannini, B. Gobbo, G. Musolino

Dipartimento di Fisica, Università di Trieste e INFN Sezione di Trieste, 34127 Trieste, Italy

J. Rothberg, S. Wasserbaech

Experimental Elementary Particle Physics, University of Washington, WA 98195 Seattle, U.S.A.

S.R. Armstrong, P. Elmer, Z. Feng,[27] D.P.S. Ferguson, Y.S. Gao,[28] S. González, J. Grahl, T.C. Greening, O.J. Hayes, H. Hu, P.A. McNamara III, J.M. Nachtman, W. Orejudos, Y.B. Pan, Y. Saadi, I.J. Scott, A.M. Walsh,[29] Sau Lan Wu, X. Wu, J.M. Yamartino, M. Zheng, G. Zobernig

Department of Physics, University of Wisconsin, Madison, WI 53706, USA[11]

[1] Now at CERN, 1211 Geneva 23, Switzerland.
[2] Supported by Dirección General de Investigación Científica y Técnica, Spain.
[3] Now at Dipartimento di Fisica, Università di Lecce, 73100 Lecce, Italy.
[4] Also Istituto di Fisica Generale, Università di Torino, Torino, Italy.
[5] Also Istituto di Cosmo-Geofisica del C.N.R., Torino, Italy.
[6] Supported by the Commission of the European Communities, contract ERBCHBICT941234.
[7] Supported by CICYT, Spain.
[8] Supported by the National Science Foundation of China.
[9] Supported by the Danish Natural Science Research Council.
[10] Supported by the UK Particle Physics and Astronomy Research Council.
[11] Supported by the US Department of Energy, grant DE-FG0295-ER40896.
[12] Now at Dragon Systems, Newton, MA 02160, U.S.A.
[13] Supported by the US Department of Energy, contract DE-FG05-92ER40742.
[14] Supported by the US Department of Energy, contract DE-FC05-85ER250000.
[15] Permanent address: Universitat de Barcelona, 08208 Barcelona, Spain.
[16] Supported by the Bundesministerium für Forschung und Technologie, Fed. Rep. of Germany.
[17] Supported by the Direction des Sciences de la Matière, C.E.A.
[18] Supported by Fonds zur Förderung der wissenschaftlichen Forschung, Austria.
[19] Permanent address: Kangnung National University, Kangnung, Korea.
[20] Now at DESY, Hamburg, Germany.
[21] Also at CERN, 1211 Geneva 23, Switzerland.
[22] Supported by the US Department of Energy, grant DE-FG03-92ER40689.
[23] Now at Wayne State University, Detroit, MI 48202, USA.
[24] Now at Max-Plank-Institüt für Kernphysik, Heidelberg, Germany.
[25] Also at Istituto di Matematica e Fisica, Università di Sassari, Sassari, Italy.
[26] Permanent address: Sung Kyun Kwon University, Suwon, Korea.
[27] Now at The Johns Hopkins University, Baltimore, MD 21218, U.S.A.
[28] Now at Harvard University, Cambridge, MA 02138, U.S.A.
[29] Now at Rutgers University, Piscataway, NJ 08855-0849, U.S.A.

1 Introduction

The Standard Model predicts only negligible $\mathcal{CP}$ violating effects in decays of the Z into quarks or leptons, as the $\mathcal{CP}$ violating contributions to these amplitudes are at most of the order of 10^{-7} [1] relative to the respective electroweak amplitudes. Therefore, a search for $\mathcal{CP}$ violation at the Z resonance is a test for physics beyond the Standard Model. Simple extensions [2] of the Standard Model with $\mathcal{CP}$-odd and $\mathcal{CP}$-even Higgs states, which could mix to build non-$\mathcal{CP}$ eigenstates, are expected to contain $\mathcal{CP}$ violating terms. As couplings of Higgs particles are functions of the masses of the interacting particles, decays with heavy quarks, especially b quarks, deserve special interest.

In this analysis a search for $\mathcal{CP}$ violating anomalous couplings is performed, as proposed by the authors of [1] and [3]. Related searches in the decay $Z \to \tau^+\tau^-$ have been already carried out, leading to an upper limit on the weak dipole form factor of the τ lepton [4].

2 Theoretical Framework

In [3] $\mathcal{CP}$-odd couplings are introduced in a model independent way using an effective Lagrangian. The Standard Model Lagrangian density $\mathcal{L}_{SM}(x)$ is extended to include all $\mathcal{CP}$-odd local operators that can be constructed with Standard Model fields, up to the mass dimension $d = 6$:

$$\mathcal{L}(\S) = \mathcal{L}_{\mathcal{SM}}(\S) + \mathcal{L}_{\mathcal{CP}}(x). \tag{1}$$

Effects in $Z \to b\bar{b}$ from $\mathcal{CP}$ violating dipole form factors would require the measurement of the spin directions of the quarks. As for quarks no spin analyzers exist, the search for $\mathcal{CP}$ violation is restricted to the analysis of the $\mathcal{CP}$-odd operator at the vertex $Z \to b\bar{b}g$, which is given by:

$$\mathcal{L}_{\mathcal{CP}}(x) \quad = [h_{Vb}\bar{b}(x)T^a\gamma^\nu b(x) + h_{Ab}\bar{b}(x)T^a\gamma^\nu\gamma_5 b(x)]Z^\mu(x)G^a_{\mu\nu}(x)\,, \tag{2}$$

where $b(x)$ denotes the b quark field, T^a are the generators of $SU_c(3)$, and $Z^\mu(x)$, $G^a_{\mu\nu}(x)$ are the fields of the Z boson and the gluon, respectively. The $\mathcal{CP}$-odd couplings at the vertex (fig. 1) are described by an axial vector part h_{Ab} and a vector part h_{Vb}. In [1] and [3] it is shown that all $\mathcal{CP}$-odd effects are proportional to the dimensionless coupling $\hat{h}_b$:

$$\hat{h}_b = \hat{h}_{Ab}g_{Vb} - \hat{h}_{Vb}g_{Ab} \tag{3}$$

with

$$\hat{h}_{Ab/Vb} = h_{Ab/Vb}\frac{\sin\vartheta_W\cos\vartheta_W m_Z^2}{eg_s}\,,$$

where g_s is the strong coupling and g_{Vb}, g_{Ab} are the Standard Model vector and axial vector couplings of the b quark to the Z.

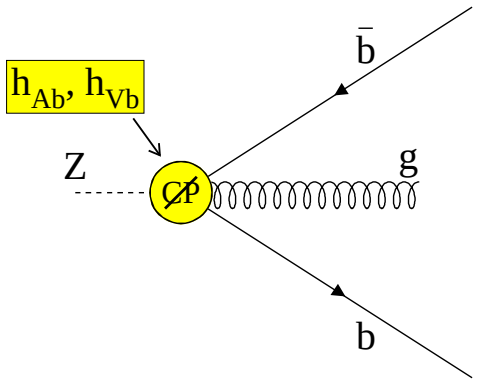

Figure 1: Anomalous couplings h_{Ab}, h_{Vb} at the vertex $Z \to b\bar{b}g$.

In a first study, $\mathcal{CP}$-odd variables are analyzed, probing the coupling $\hat{h}_b$. To measure $\hat{h}_b$ the $\mathcal{CP}$-odd tensor T'_{ij} [3] is used:

$$T'_{ij} = (\hat{k}_{\bar{q}} - \hat{k}_q)_i \left(\frac{\hat{k}_{\bar{q}} \times \hat{k}_q}{| \hat{k}_{\bar{q}} \times \hat{k}_q |} \right)_j + (i \leftrightarrow j)\,, \tag{4}$$

where $\hat{k}_q$, $\hat{k}_{\bar{q}}$ denote the normalized momentum vectors of the quark and anti-quark, respectively, and i, j are the cartesian coordinates. The tensor T'_{ij} is symmetric in i and j, traceless, and invariant when exchanging $\hat{k}_q$ and $\hat{k}_{\bar{q}}$. Therefore an identification of the quark and anti-quark jet is not necessary: only the gluon jet has to be tagged. If $\mathcal{CP}$ invariance holds, the mean values of the tensor elements are zero, i. e., $\langle T'_{ij} \rangle \neq 0$ indicates $\mathcal{CP}$ violation. In the case of $\mathcal{CP}$-odd couplings $\langle T'_{ij} \rangle$ is proportional to the tensor polarization s_{ij} of the Z boson (see eq. 3.20 in [1]). At LEP s_{ij} is a diagonal tensor:

$$s_{ij} = \mathrm{diag}(-\frac{1}{6}, -\frac{1}{6}, \frac{1}{3})\,. \tag{5}$$

Since $\langle T'_{33} \rangle$ is the most sensitive observable (see eq. 5) and totally correlated to $\langle T'_{11} \rangle$ and $\langle T'_{22} \rangle$ it is the only one used to determine $\hat{h}_b$. In [3] it is shown that $\mathcal{CP}$-odd effects caused by the coupling introduced in eq. 2 are proportional to $\hat{h}_b$:

$$\langle T'_{33} \rangle = \hat{h}_b Y'\,. \tag{6}$$

The sensitivity Y' is a constant derived by integration of the experimentally accessible phase space. The effect of a $\mathcal{CP}$ violating coupling on T'_{33} is illustrated in fig. 2 a).

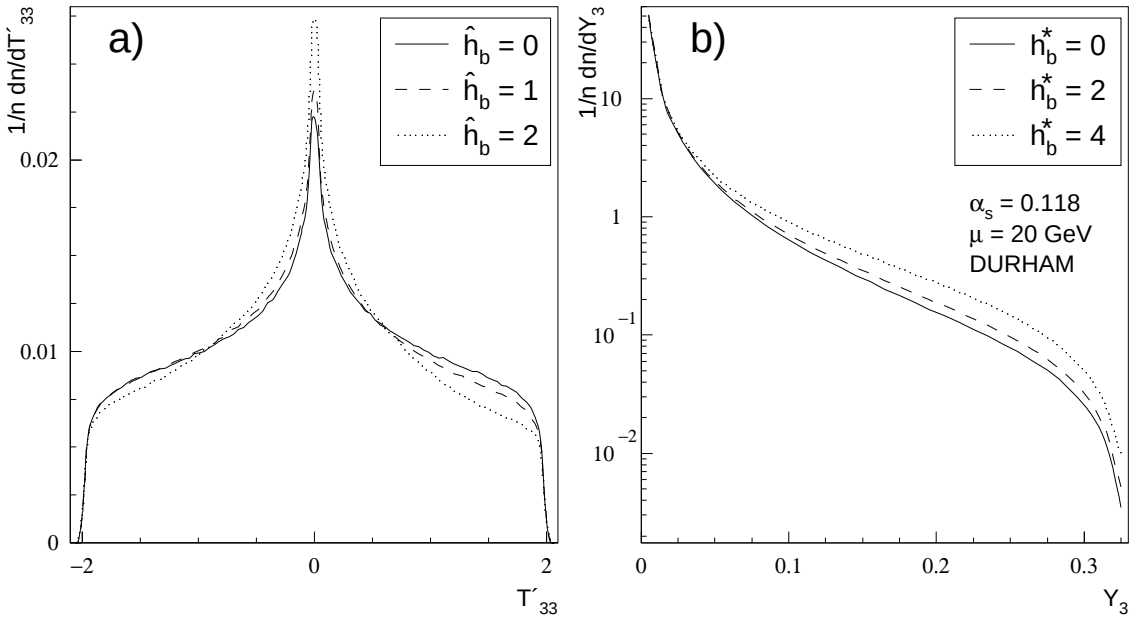

Figure 2: Observables of both measurements, T'_{33} (only b quarks) and $D_2(Y_3) = 1/n\ dn(Y_3)/dY_3$ at the parton level, with and without $\mathcal{CP}$-odd couplings.

In a subsequent analysis, additional contributions from anomalous couplings to the three-jet rate in the process $Z \to b\bar{b}g$ have been searched for. Such additional contributions are proportional to the combination h_b^{*2}, with

$$h_b^* = \sqrt{\hat{h}_{Vb}^2 + \hat{h}_{Ab}^2}\,, \tag{7}$$

and would manifest themselves in a higher value of the strong coupling constant for b quarks, $\alpha_s^b(M_Z^2)$. Therefore, assuming flavour independence of α_s i.e. $\alpha_s^b/\alpha_s^{udsc} = 1$, and assigning any deviation of this ratio to these new couplings, an upper limit on h_b^* can be given. In this respect the analysis is complementary but correlated to that of [5], where the flavour independence of α_s has been studied without the assumption of $\mathcal{CP}$ violating couplings.

The analysis of h_b^* is based on the differential two-jet rate D_2 (see fig. 2 b), which is the normalized distribution of the event shape variable Y_3, $D_2(Y_3) = 1/\sigma\ d\sigma(Y_3)/dY_3$, with Y_3 being the $y_{\rm cut}$ at which an event changes its classification from three jets to two jets. The differential two-jet rate has been computed using perturbation theory up to $\mathcal{O}(\alpha_f^{\in})$. Instead of analyzing D_2 directly, the ratio $R^{\rm exp}$ of the distribution of a b-enriched sample and the distribution of an inclusive hadronic sample is measured. The experimental observable $R^{\rm exp}$ is defined as follows:

$$R^{\rm exp} = \frac{D_2^{b\,\rm tag}(Y_3)}{D_2^{\rm incl}(Y_3)}\,. \tag{8}$$

It has been shown [5], that some of the theoretical and experimental uncertainties cancel in this ratio. The theoretical description $R^{\rm th}$, which depends on h_b^*, is developed in section 5.

Additional couplings at the vertex $Z \to b\bar{b}g$ could also contribute to the partial width $\Gamma_{b\bar{b}}$, thus possibly enhancing R_b beyond its Standard Model value. In [3] the possible impact of these couplings on R_b is discussed. By attributing the observed deviation of $R_b^{exp} = 0.2209 \pm 0.0021$ [6] from the Standard Model expectation $R_b = 0.2155 \pm 0.0005$ [7] entirely to these anomalous couplings, a value of $h_b^* = 1.93 \pm 0.75$ can be calculated. It should be stressed, however, that even if R_b agreed with the Standard Model value, $\mathcal{CP}$ violation of the kind described here is not excluded, because possible interferences could cancel the effect on the width.

3 Detector and Data Sample

The ALEPH detector is described in detail in [8] and its performance in [9]. Only a brief description of the components used in this analysis is given here. A high resolution vertex detector, consisting of two layers of double sided silicon microstrip detectors is the innermost of the tracking devices. Each layer provides measurements in both the $r\phi$ and rz views at average radii of 6.3 and 10.8 cm, with a spatial resolution of 12 μm in $r\phi$ and, depending on the track polar angle, between 12 and 22 μm for the z coordinate. The inner and the outer layers cover 85% and 69% of the solid angle. The vertex detector is surrounded by the Inner Tracking Chamber (ITC) and the Time Projection Chamber (TPC). The ITC is a cylindrical drift chamber which provides up to 8 points per track in the $r\phi$ view at radii from 16 to 26 cm. The TPC reconstructs up to 21 space points per track at radii between 40 and 171 cm. The tracking detectors are immersed in an axial magnetic field of 1.5 Tesla, providing a measurement of the momentum of charged particles with a resolution $\delta p_t/p_t = 0.0006 p_t \oplus 0.005$ (p_t in GeV/c). The electromagnetic calorimeter (ECAL), which surrounds the TPC and which is completely contained within the superconducting coil of the magnet, is a lead proportional tube calorimeter, segmented into $0.9^\circ \times 0.9^\circ$ projective towers and read out in three separate longitudinal stacks. The calorimeter is used to measure the electromagnetic energy with a resolution of $\sigma(E)/E = 18\%/\sqrt{E[\mathrm{GeV}]} + 0.009$ and, together with the TPC, to identify electrons. The hadron calorimeter (HCAL) is composed of the iron of the magnet return yoke interleaved with 23 layers of streamer tubes and is surrounded by two double layers of streamer tubes to enhance the identification of muons.

Hadronic events are selected requiring at least 6 well measured tracks, their total energy exceeding 15 GeV. A track is defined as well measured when the angle to the beam axis is greater then 18.2°, there are at least four TPC points used for the fit of the track, and it passes through a cylinder centered around the fitted interaction point with a radius of 2 cm and a length of 10 cm. The total visible energy of neutral and charged particles must exceed 45 GeV. The selection efficiency is 91%, and the background is about 0.2 % stemming from $Z \to \tau^+\tau^-$ and two-photon events. After these cuts about 2.7×10^6 hadronic events recorded in 1991 to 1994 remain for further analysis.

Jets are defined using the JADE [10] and Durham [11] metrics $y^{\mathrm{J}}_{ij} = E_i E_j (1 - \cos\theta_{ij})/E^2_{\mathrm{vis}}$ and $y^{\mathrm{D}}_{ij} = 2\min(E_i^2, E_j^2)(1 - \cos\theta_{ij})/E^2_{\mathrm{vis}}$, where E^2_{vis} indicates the visible energy and i, j are the indices of charged tracks and neutral objects reconstructed by the ALEPH tracking system and the calorimeters. In the $\hat{h}_b$ analysis the JADE algorithm with a fixed cut off value of $y_{\mathrm{cut}} = 0.03$ is used. In the h_b^* analysis both jet schemes are employed to measure the differential two-jet rate $D_2(Y_3)$.

In both analyses, b events are selected exploiting the sizeable impact parameters due to b decays. The b tagging algorithm, described in detail in reference [12], first reconstructs the primary vertex of the event. Then the probability for each charged particle to originate from the primary vertex is calculated using the track impact parameter. They are combined into probabilities $\mathcal{P}$ associated to sets of tracks like jets ($\mathcal{P}_{\mathcal{J}}$) or whole events ($\mathcal{P}_{\mathcal{E}}$). In both analyses b events are selected with a cut on the event probability $\mathcal{P}_{\mathcal{E}}$, resulting in b purities of more than 85%. After the b tagging, the two analyses follow different approaches and will be described separately.

4 Analysis of Anomalous Couplings from $Z \to b\bar{b}g$ Topologies

In the study of $\mathcal{CP}$-odd contributions three-jet events are selected. These events are retained if the jets consist of at least three particles, two of them being charged tracks, the visible energy of the jets exceeds 5 GeV, the angle between jet and beam is larger than 26°, and the aplanarity of the whole event is less than 0.05. These cuts are applied to ensure a good reconstruction of the jets.

The energy resolution of the jets is enhanced by exploiting the angular reconstruction of charged and neutral particles. Assuming massless jets, the jet energies $E_{\mathrm{jet\,i}}$ are recalculated by using the jet directions

$$E_{\mathrm{Jet\,i}} = E_{\mathrm{cm}} \frac{\sin\alpha_{jk}}{\sin\alpha_{ij} + \sin\alpha_{jk} + \sin\alpha_{ki}}\,, \tag{9}$$

where α_{ij} is the angle between jet i and j. Then the energies of the reconstructed jets are ordered, $E_{\mathrm{jet\,1}} > E_{\mathrm{jet\,2}} > E_{\mathrm{jet\,3}}$. As mentioned in section 2, only the gluon jet has to be tagged. Selecting the lowest energy jet as the gluon jet candidate represents a gluon tag referred to as an "energy tag". In a further step, which is only possible in the b sample, energy ordering and lifetime information are combined. The gluon jet candidate is selected using the probability $\mathcal{P}_{\mathcal{J}}$ of the individual jets: from the two lower energy jets, the jet with the higher $\mathcal{P}_{\mathcal{J}}$ is chosen as the gluon jet candidate. This tag will be called a "lifetime" tag. Besides having a higher purity, the main advantage of the lifetime tag compared to the energy tag is the possibility to tag gluon jets up to energies of 40 GeV. This is important, as the sensitivity Y' increases with the energy of the gluon jet.

The purity of the sample, defined as the ratio of correctly tagged gluons in $b\bar{b}g$ events over all selected events, is estimated using simulated events generated with JETSET [13]. Jets are defined at parton and hadron levels by clustering final state partons and hadrons with a y_{cut} of 0.03. If the number of parton and hadron jets agrees, it is considered to be the true number of jets, otherwise the event is ambiguous and discarded in the further analysis. In the case of a so defined three-jet event, the jet containing neither the primary quark nor the anti-quark is regarded as gluon jet. If three jets are found after the simulation of the detector response, the reconstructed jets are matched to their mother partons by forming pairs with least angular separation. Events are classified as correctly matched if the largest separation angle is less than 26°. The jets at hadron level are matched in the same way. If one of these criteria fails, these events are ambiguous and rejected. Events with n jets at the parton and hadron levels and three reconstructed jets are classified as n-jet background. The described matching procedure is chosen in order to get clearly defined three-jet events, but it is still arbitrary to a certain extent. To estimate the systematic error on the purity, a different matching procedure is chosen, ignoring the hadron level and omitting the cut on the separation angle. In this second procedure no event is classified as ambiguous, i. e., all simulated events are used to estimate the purity. The difference in the purities obtained by these two definitions is used as the systematic uncertainty due to the matching procedure (see table 1).

With the lifetime tag a purity of about 74% is achieved. The complete composition of the selected sample is shown in table 1. The efficiency, defined as selected $b\bar{b}g$ events with successfully tagged gluon compared to the total rate of $Z \to b\bar{b}g$ events, is about 19%. This number is obtained by defining true $b\bar{b}g$ events as above, i. e. with a y_{cut} of 0.03 at parton and hadron levels.

composition	uds quarks	c quarks	b quarks
two-jet background	$0.1\pm0.1\pm0.1$	$0.5\pm0.1\pm0.1$	$8.5\pm0.2\pm0.5$
four-jet background	$0.1\pm0.2\pm0.1$	$0.3\pm0.1\pm0.1$	$3.2\pm0.2\pm0.2$
three-jet, mistagged gluon	$0.7\pm0.1\pm0.1$	$0.8\pm0.2\pm0.2$	$8.0\pm0.2\pm0.2$
three-jet, tagged gluon	$0.2\pm0.1\pm0.1$	$4.0\pm0.2\pm0.1$	$73.6\pm0.4\pm0.9$

Table 1: Composition of the selected sample for the lifetime tag. All numbers are given in percent, the first error is the statistical one, the second error is the systematic uncertainty due to the different matching procedures.

The measurement is performed on the data collected until 1994. After applying the data selection, a sample of 85342 $b\bar{b}g$ candidates remains for the T'_{ij} measurement. The mean values

$\langle T'_{ij} \rangle$ are shown in table 2. No indication of $\mathcal{CP}$ violation nor fake effects are observed.

data sample	$\langle T'_{ij} \rangle$ [$\times 10^{-3}$]		
b quarks, lifetime tag	-3.4 ± 3.6	-1.2 ± 3.1	-0.7 ± 3.1
		3.9 ± 3.6	-1.3 ± 2.9
			-0.5 ± 3.7
b quarks, energy tag	-2.9 ± 3.6	-2.1 ± 3.1	-3.1 ± 3.1
		4.3 ± 3.6	-5.0 ± 2.9
			-1.4 ± 3.7
light quarks, energy tag	0.7 ± 2.1	-2.7 ± 1.7	-0.7 ± 1.9
		0.2 ± 2.6	-1.3 ± 1.6
			-0.9 ± 3.1

Table 2: Result of $\langle T'_{ij} \rangle$ of different data samples and tagging methods. Only statistical errors are given here.

The measurement is also performed on a sample enriched with light quarks to ensure that no effect due to the selection mechanism is present and to check the assumption that no $\mathcal{CP}$ violating effect exists in events with light quarks. Light flavours are selected with the cut $\mathcal{P}_\mathcal{E} > 1.\bigtriangledown$. The gluon jet in these events is tagged with the energy tag. In table 2 the b-enriched and the light quark samples are compared, using the same tagging method in both samples. The comparison between b quarks and light quarks shows no significant discrepancy between the two completely independent samples. Hence it is concluded that no significant fake $\mathcal{CP}$ violating effect due to the selection is present.

4.1 Systematic Errors of the Measurement

The systematic uncertainties are estimated by studying the influence of the data selection and possible detector asymmetries. The systematic uncertainties are listed in table 3.

To estimate the effect of the selection cuts, all the cuts are varied in a wide range. The cuts of the event selection have only a very small influence on the selected sample compared to the cuts to select well-defined three-jet configurations ($y_{\rm cut}$, aplanarity, jet energies, multiplicities and angles). Therefore, the systematic error is estimated using these cuts only, by adding the uncertainties of the individual cuts in quadrature.

The $\mathcal{CP}$ invariance of the b tag is checked by dividing the three-jet sample into disjoint subsamples with different $\mathcal{P}_\mathcal{E}$ values. Using these subsamples, a sample of $\langle T'_{33} \rangle$ values is measured to test the bias of the $\mathcal{P}_{\rm E}$ cut. The $\langle T'_{33} \rangle$ values are found to be well compatible with statistical fluctuations. The uncertainty is estimated from a Gaussian fit to the distribution.

The background, summarized in table 1, is checked with Monte Carlo and found to be $\mathcal{CP}$-even. The observed uncertainty is negligible and not taken into account.

The influence of the detector on the measurement is checked in different ways. The observable $\langle T'_{33} \rangle$ is measured in control samples consisting of all three-jet events (no cut on $\mathcal{P}_\mathcal{E}$) and all two-jets events, in both cases without significant effect. Detector asymmetries faking $\mathcal{CP}$ violation, like rotations of one detector side with respect to the other are simulated. Such asymmetries, as observed, e. g., in $\mu^+\mu^-$ events [4], are found to be too small to cause any significant effect on the jet directions. The $\mathcal{CP}$ symmetry of the detector is estimated by measuring $\langle T'_{33} \rangle$ on a sample of track pairs in hadronic events. This sample is selected by dividing every accepted hadronic event into two hemispheres perpendicular to the thrust axis. The track pairs are formed by choosing one track from each hemisphere. The resulting asymmetry is compatible with zero within one standard deviation, and the mean of this measurement is taken as the systematic uncertainty.

The quality of the reconstruction of the jet direction is estimated by measuring the difference of the $\langle T'_{33} \rangle$ at the parton level and after the full detector simulation. The error is derived from the width of the difference distribution.

source of systematic error	$\Delta T'_{33}\,[\times 10^{-3}]$
$y_{\rm cut}$	± 1.8
aplanarity cut	± 1.4
$\cos\theta$ cut	± 0.6
charged multiplicity	± 0.6
total multiplicity cut	± 1.0
energy cut	± 1.2
b tag	± 1.1
detector symmetry	± 0.8
jet resolution	± 0.7
total systematic error	± 3.3

Table 3: Systematic errors of the $\langle T'_{33} \rangle$ measurement.

4.2 Determination of $\hat{h}_b$

To extract the coupling $\hat{h}_b$ from the measurement of $\langle T'_{33} \rangle$ the effective sensitivity Y' has to be calculated. This has been done by means of a Monte Carlo generator [14], which includes the $\mathcal{CP}$ violating couplings characterized by eq. 2. Each measured three jet configuration is weighted for different values of $\hat{h}_b$ taking the energy dependence of the tagging purity and the background into account. With this procedure a reweighted $\langle T'_{33} \rangle$ is calculated for each value of $\hat{h}_b$. The sensitivity of the data selection is given by the $\hat{h}_b$ dependence of the reweighted $\langle T'_{33} \rangle$ values. The calculated sensitivity $Y' = -0.0167 \pm 0.0002_{\rm stat}$ is constant, showing no dependence on $\hat{h}_b$.

The systematic errors on the sensitivity stem from the errors on the tagging purity and from the influence of the b quark mass. The former have been estimated by varying the purity within its uncertainties and recalculating Y'. In this way the statistical errors due to the gluon tagging purity, the systematic error on the the purity definition (see table 1) and systematic uncertainties in the b purity are considered. The largest error is caused by the dependence of the sensitivity on the b quark mass [15]. The systematic errors are summarized in table 4.

source of systematic error	$\Delta Y'$
statistical error on the gluon purity	± 0.0004
systematic error on the b purity	± 0.0007
systematic error on the gluon purity	± 0.0002
b mass effects	± 0.0013
total systematic error	± 0.0015

Table 4: Systematic errors on the sensitivity Y'.

The sensitivity of the data selection is given by

$$Y' = -0.0167 \pm 0.0002_{\rm stat} \pm 0.0015_{\rm syst}\,.$$

4.3 Results of the $\hat{h}_b$ Analysis

Taking the systematic errors into account the measurement of the $\mathcal{CP}$-odd observable in a sample of $Z \to b\bar{b}g$ events yields:

$$\langle T'_{33} \rangle = (-0.5 \pm 3.7_{\text{stat}} \pm 3.3_{\text{syst}}) \times 10^{-3} .$$

The measurement is consistent with $\langle T'_{33} \rangle = 0$, hence no evidence for $\mathcal{CP}$ violation in $Z \to b\bar{b}g$ has been found. The size of the $\mathcal{CP}$-odd coupling $\hat{h}_b$ is extracted using eq. 6:

$$\hat{h}_b = 0.03 \pm 0.22_{\text{stat}} \pm 0.20_{\text{syst}} .$$

From this measurement a limit on the coupling of $| \hat{h}_b | < 0.59$ (95% CL) is derived.

5 Measurement of Anomalous Couplings from the Differential Two-Jet Rate

Of all the event shape variables studied in [5], only for Y_3 theoretical calculations including anomalous couplings are available [15]. Therefore, the second analysis concentrates on possible additional contributions to the differential two-jet rate $D_2(Y_3)$ due to the anomalous coupling h_b^*. The theoretical prediction for $D_2(Y_3)$ is given by

$$\begin{aligned} D_2(Y_3) &= \frac{\alpha_s(\mu^2)}{2\pi} A(Y_3) + \left(\frac{\alpha_s(\mu^2)}{2\pi}\right)^2 \left[A(Y_3) 2\pi b_0 \ln\left(\frac{\mu^2}{M_Z^2}\right) + B(Y_3) \right] \qquad (10) \\ b_0 &= \frac{33 - 2n_f}{12\pi} \end{aligned}$$

where μ is the renormalization scale, and the coefficients A and B have been computed to second order of perturbative QCD [16]. Here $h_b^* \gg h_{udsc}^*$ is assumed. Hence the prediction for *udsc* quarks in eq. 10 is entirely fixed by the Standard Model and does not depend on h^*. In contrast, D_2 for b quarks receives contributions from new physics and the prediction is modified by an additional term proportional to h_b^{*2}:

$$\begin{aligned} D_2^b(Y_3) &= \frac{\alpha_s(\mu^2)}{2\pi} \left(A'(Y_3) + h_b^{*2} C'(Y_3) \right) \\ &\quad + \left(\frac{\alpha_s(\mu^2)}{2\pi}\right)^2 \left[A'(Y_3) 2\pi b_0 \ln\left(\frac{\mu^2}{M_Z^2}\right) + B'(Y_3) \right] . \qquad (11) \end{aligned}$$

Note that the coefficients A' and B' are different from those in eq. 10, because the total cross section needed for normalization is changed if anomalous couplings are present. Contributions from dipole form factors are expected to be suppressed [1, 3] and have been assumed to be zero in the normalization. The coefficient C' has been calculated to leading order [15].

Based on eq. 10 and eq. 11, a theoretical description R^{th} of the observable can be derived:

$$R^{th} = \frac{P_b D_2^{b,b\,\text{tag}}(Y_3) + (1 - P_b) D_2^{udsc,b\,\text{tag}}(Y_3)}{R_b D_2^{b\,\text{incl}}(Y_3) + (1 - R_b) D_2^{udsc\,\text{incl}}(Y_3)} , \qquad (12)$$

where P_b is the purity of the lifetime-enriched b sample, R_b is the fraction of Z's decaying into b quarks and $D_2^{q\,tag}$ stands for the distribution of a flavour q in a sample of type *tag*. These distributions are constructed from the parton level predictions and have to be corrected for the following effects: mass corrections for b quarks, initial and final state radiation, hadronization effects, the detector acceptance, the influence of the detector resolution, and the tagging bias. After applying these corrections to R^{th}, a value of h_b^* is extracted from a binned least-square fit to the data (see fig. 3).

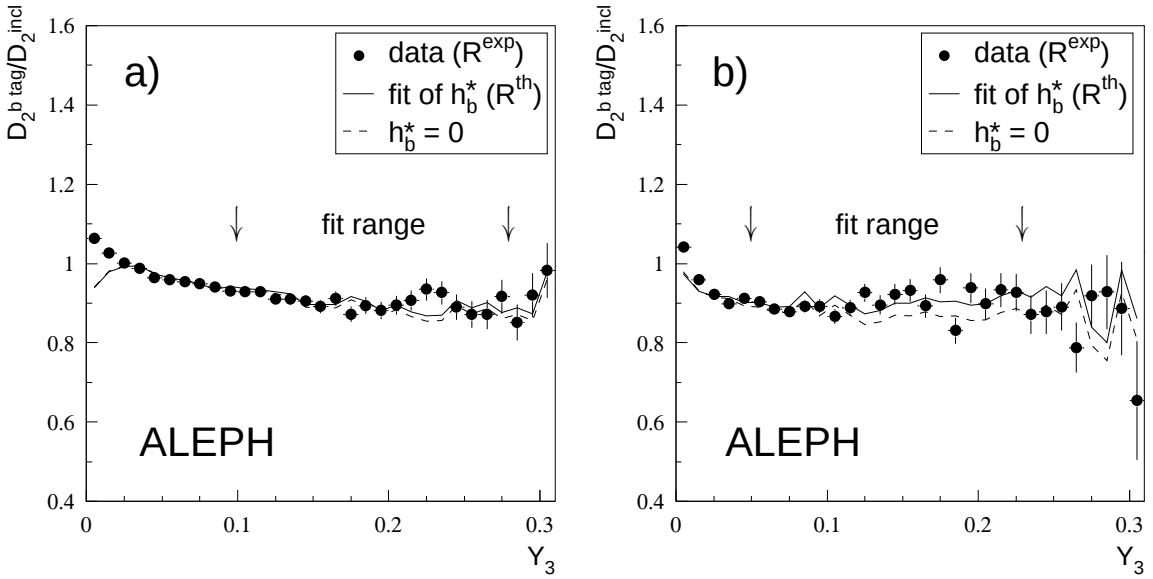

Figure 3: Fit of the theoretical description R^{th} to the experimental observable R^{exp}. Figure a) shows the result for the JADE algorithm ($h_b^* = 0.80 \pm 0.33$, $\chi^2 = 10.6$, $d.o.f. = 18$), and figure b) depicts the result with the Durham algorithm ($h_b^* = 1.19 \pm 0.25$, $\chi^2 = 8.0$, $d.o.f. = 17$). The hadronization corrections are made with the matrix element model (ME). Included are also the expectations for $h_b^* = 0$.

5.1 Determination of h_b^* and Systematic Errors

The fit function $R^{\rm th}$ depends explicitly on h_b^*, α_s and μ. The value of the strong coupling constant is set in the fit function to $\alpha_s(M_Z^2) = 0.118$ and is varied by ± 0.007. The renormalization scale is set to 15 GeV. This symmetrizes the error from the scale uncertainty, which is varied from $\mu = m_b$ to $\mu = M_Z$.

The fit range ($Y_3 = 0.10$–0.28 for the JADE algorithm and $Y_3 = 0.05$–0.23 for the Durham algorithm) is chosen to optimize the sensitivity and to guarantee a good perturbative description, i. e., at large Y_3 where the hadronization and mass corrections are small. Since this choice is not unique, the fit is repeated with a range modified by two bins ($\Delta Y_3 = 0.02$).

Jets are reconstructed using charged tracks and neutral calorimeter objects. The uncertainty of the reconstruction procedure is estimated by repeating the analysis with charged tracks only.

The b sample is enriched by means of a lifetime tag, which leads to a distortion of the differential two-jet rate of less than 10%. Therefore, a correction is elaborated using full detector simulation. The stability of these corrections is checked by varying the lifetime cuts in the data resulting in a change of the purity of the sample of 10%. The same cuts are applied to the simulated data and the corrections for the tagging bias recalculated.

The b quark fragmentation is described by the fragmentation function of Peterson et al. [17]. The main parameter of this function is ϵ_b, measured to be $\epsilon_b = (3.2 \pm 1.7) \times 10^{-3}$ [18]. Monte Carlo simulations with a corresponding range of values are done to study the effect on h_b^*.

An important source of uncertainty is related to mass corrections. These have been calculated in [19] at tree level. These calculations are only complete to $\mathcal{O}(\alpha_s)$ and are applied to the coefficient A' in eq. 11. The uncertainty on the b quark mass is set to 0.5 GeV/c^2 and the corresponding correction recalculated.

In order to account for missing higher orders, the available $\mathcal{O}(\alpha_s^2)$ four-jet computation is used for correction as well and the difference to the $\mathcal{O}(\alpha_s)$ result taken as systematic error.

Finally, the parameters R_b and P_b are varied in the fit function within their errors and an error on the normalization is derived. Typical systematic uncertainties for the two cluster algorithms, JADE and Durham, are summarized in table 5 (the exact value of the errors is weakly dependent on the hadronization models).

source	JADE	DURHAM
α_s	± 0.02	± 0.01
μ	± 0.22	± 0.27
m_b	± 0.06	± 0.07
mass corr.	± 0.25	± 0.22
ϵ_b	± 0.12	± 0.11
fit range	± 0.02	± 0.04
det. res.	± 0.12	± 0.03
tag. bias	± 0.06	± 0.07
R_b	± 0.02	± 0.02
P_b	± 0.05	± 0.04
norm.	± 0.03	± 0.02
systematic uncertainty	± 0.38	± 0.37

Table 5: Typical systematic uncertainties on h_b^* for the two jet algorithms JADE and Durham.

5.2 Hadronization Model Uncertainty and Results of the h_b^* Analysis

The main theoretical uncertainty is caused by the hadronization of partons to physical hadrons. To estimate the uncertainty due to the hadronization model, the results achieved with four different generators are compared: the matrix element with string fragmentation (ME), the parton shower (Q_0 = 1 GeV, Q_0 being the cut-off of the parton shower) as implemented in JETSET [13] with string fragmentation (PS), the model of cluster fragmentation in HERWIG [20] (HW) and the dipole cascade model implemented in ARIADNE [21] (AR).

The results of the fit to the data are given in table 6 for each hadronization model separately. The linear correlation coefficient between the JADE and the Durham analysis is estimated to 68%. Using this correlation, a combined result for each hadronization model can be derived which minimizes the total statistical error.

Model	JADE	Durham	combined
ME	$0.80 \pm 0.33 \pm 0.45$	$1.19 \pm 0.25 \pm 0.42$	$1.05 \pm 0.26 \pm 0.40$
AR	$0.75 \pm 0.30 \pm 0.45$	$0.85 \pm 0.37 \pm 0.41$	$0.79 \pm 0.30 \pm 0.40$
PS	$1.80 \pm 0.16 \pm 0.38$	$1.67 \pm 0.19 \pm 0.37$	$1.75 \pm 0.16 \pm 0.35$
HW	$1.81 \pm 0.16 \pm 0.39$	$1.77 \pm 0.19 \pm 0.39$	$1.79 \pm 0.16 \pm 0.36$

Table 6: Results on h_b^* from the least-square fit for four different hadronization models. The first error is the statistical one, the second the total systematic uncertainty.

After averaging the combined results of the different hadronization models the following result ist obtained:

$$h_b^* = 1.34 \pm 0.22_{\mathrm{stat}} \pm 0.38_{\mathrm{syst}} \pm 0.50_{\mathrm{hadr}} \, .$$

where the first error is the statistical one, the second error contains all systematic uncertainties but the hadronization model and the last one reflects the systematic uncertainty due to the hadronization model itself. The upper limit is derived by adding linearly the systematic and statistical errors:

$$h_b^* < 3.02 \ (95\% \ \mathrm{CL}) \, .$$

6 Conclusions

A search for $\mathcal{CP}$ violation beyond the standard model in the decay $Z \to b\bar{b}g$ has been performed. Two combinations of $\mathcal{CP}$-odd couplings, namely h_b^* and $\hat{h}_b$ have been analyzed. No evidence for $\mathcal{CP}$-odd couplings is found in both analyses. The derived limit on h_b^* is consistent with the value calculated from the R_b measurement.

Using eq. 3 and eq. 7, the two measurements presented in this paper can be used to constrain the couplings h_{Ab}, h_{Vb}. In fig. 4 the 95% CL limits of both measurements on h_{Ab} and h_{Vb} are shown, being well consistent with each other.

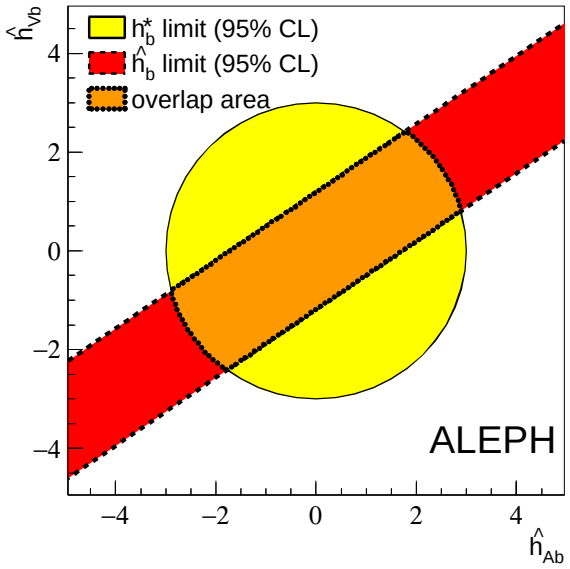

Figure 4: Combined results. The shaded areas depict the constraints of the measurements on the couplings $\hat{h}_{Ab}$ and $\hat{h}_{Vb}$.

Acknowledgments

We would like to acknowledge the continuous interest and the helpful support of W. Bernreuther, P. Haberl and O. Nachtmann in this work. We wish to thank our colleagues from the CERN accelerator divisions for the successful operation of LEP. We are indebted to the engineers and technicians in all our institutions for their contribution to the good performance of ALEPH. Those of us from non-member states thank CERN for its hospitality.

References

[1] W. Bernreuther, U. Löw, J. P. Ma, and O. Nachtmann, Z. Phys. **C43** (1989) 117.

[2] W. Bernreuther, T. Schröder, and T. N. Pham, Phys. Lett. **B279** (1992) 389.; S. M. Barr, A. Masiero, Phys. Rev. Lett. **187** (1987) 187; J. C. Pati, A. Salam, Phys. Rev. **D10** (1975) 275.

[3] W. Bernreuther, D. Bruß, P. Haberl, and O. Nachtmann, Z. Phys. **C68** (1995) 73.

[4] D. Buskulic et al., ALEPH Collaboration, Phys. Lett. **B297** (1992) 459; **B346** (1995) 371; P. D. Acton et al., OPAL Collaboration, Phys. Lett. **B281** (1992) 405; R. Akers et al., OPAL Collaboration, Z. Phys. **C66** (1995) 31.

[5] D. Buskulic et al., ALEPH Collaboration, Phys. Lett. **B355** (1995) 381; H. Stenzel, PhD thesis, Heidelberg, HD-IHEP 95-03 (1995); B. Adeva et al., L3 Collaboration, Phys. Lett. **B271** (1991) 461; R. Akers et al., OPAL Collaboration, Z. Phys. **C60** (1993) 397; P. Abreu et al., DELPHI Collaboration, Phys. Lett. **B307** (1993) 221; K. Abe et al., SLD Collaboration, Phys. Rev. **D53** (1996) 2271; R. Akers et al., OPAL Collaboration, Z. Phys. **C65** (1995) 31.

[6] The LEP Collaborations ALEPH, DELPHI, L3 and OPAL, CERN-PPE/96-017 (1996), subm. to Nucl. Instr. and Meth.

[7] The LEP Collaborations ALEPH, DELPHI, L3 and OPAL, CERN-PPE/95-172 (1995)

[8] D. Decamp et al., ALEPH Collaboration, Nucl. Instr. and Meth. **A294** (1990) 121.

[9] D. Buskulic et al., ALEPH Collaboration, Nucl. Instr. and Meth. **A360** (1995) 481.

[10] W. Bartel et al., JADE Collaboration, Z. Phys. **C33** (1986) 23; Phys. Lett. **B213** (1988) 235.

[11] S. Catani et al., Phys. Lett. **B269** (1991) 432; W. J. Stirling, Durham Workshop, J. Phys. **G17** (1991) 1657.

[12] D. Buskulic et al., ALEPH Collaboration, Phys. Lett. **B313** (1993) 535.

[13] T. Sjöstrand, Comp. Phys. Comm. **39** (1986) 347; **43** (1987) 367; **82** (1994) 74.

[14] W. Bernreuther, CP3JET, private communication

[15] P. Haberl, HD-THEP 96-16 (1996)

[16] Z. Kunszt et al., in "Z Physics at LEP 1", edited by G. Altarelli, CERN Yellow Report 89-08 (1989) 373.

[17] C. Peterson et al., Phys. Rev. **D27** (1983) 105.

[18] D. Buskulic et al., ALEPH Collaboration, Z. Phys. **C62** (1994) 179.

[19] A. Ballestrero et al., Phys. Lett. **B294** (1992) 425; **B323** (1994) 53; **B415** (1994) 265.

[20] G. Marchesini et al., Nucl. Phys. **B310** (1988) 571; Comp. Phys. Comm. **67** (1992) 269.

[21] L. Lönnblad, Comp. Phys. Comm. **71** (1992) 465.